Sodium channel inactivation kinetics of rat sensory and motor nerve fibres and their modulation by glutathione

N. Mitrović, S. Quasthoff, P. Grafe

Physiologisches Institut, Universität München, Pettenkoferstrasse 12, D-80336 München, Germany

Abstract. Na^+ channel currents of rat motor and sensory nerve fibres were studied with the patch-clamp technique on enzymatically demyelinated axons. Differences between motor and sensory fibres in multi-channel inactivation kinetics and the gating of late single-channel currents were investigated. In the axon-attached mode, inactivation of multi-channel Na^+ currents in sensory axons was best fitted with a single time constant while for motor axons two time constants were needed. Late single-channel currents in sensory axons were characterized by short openings whereas motor axons exhibited additional long single-channel openings. In contrast, in excised, inside-out membrane patches, no differences between motor and sensory fibres were found: in both types of fibre inactivation of multi-channel Na^+ currents proceeded with two time constants and late single-channel currents showed short and long openings. After application of the reducing agent glutathione to the cytoplasmic side of excised inside-out patches, inactivation of Na^+ currents in both motor and sensory fibres proceeded with a single, fast exponential time constant and late currents appeared with short openings only. These data indicate that the axonal metabolism may contribute to the different inactivation kinetics of Na^+ currents in motor and sensory nerve fibres.

Key words: Axon – Peripheral nerve – Patch clamp – Ion channels – Metabolism – Glutathione – Iodate – Monochlorobimane
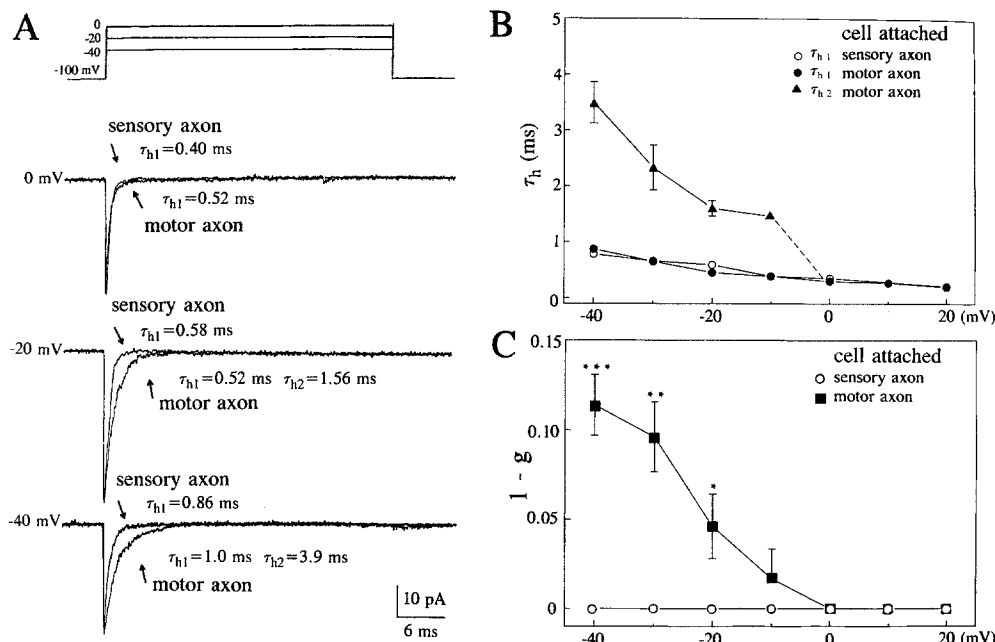
Introduction

Motor and sensory nerve fibres show distinct differences in their electrophysiological properties. These differ-

ences were first attributed to different K^+ conducting systems [13, 15]. However, after a block of K^+ currents, Bretag and Stämpfli [2] found additional differences in the Na^+ conductance inactivation since action potentials lasted longer in motor than in sensory fibres. Chiu [4] described Na^+ inactivation as a second-order process with a fast and a slow component. More recently, this finding has been confirmed by Benoit et al. [1]. Schwarz et al. [22] investigated differences in motor and sensory Na^+ current inactivation kinetics in voltage-clamped frog nerve fibres and found that development of Na^+ current inactivation was approximated by the sum of two exponentials. Motor and sensory fibres differed in the contribution of the slow and fast phase of the inactivation process. In motor nerve fibres both components contributed to inactivation throughout the potential range investigated. In sensory fibres, on the other hand, slow inactivation was absent during strong depolarizations. It was concluded that these differences in Na^+ permeability inactivation could explain the different time courses of action potentials in motor and sensory fibres when K^+ conductances are blocked.

Jonas et al. [8] developed a method of applying the patch-clamp technique [7] to myelinated nerve fibres and recorded single-channel Na^+ currents from the nodal area of demyelinated frog axons. Using this new approach, we have been able to study differences in Na^+ channel inactivation in mammalian motor and sensory nerve fibres on the multi- as well as the single-channel level. Recently we have shown that excised, inside-out axonal membrane patches from sensory nerve fibres reveal two time constants of Na^+ channel inactivation as compared to only one in axon-attached patches [24]. The slow time constant of inactivation disappeared after addition of the reducing agent glutathione (GSH) to the bathing solution [24]. In the present study we tested the possibility that differences in Na^+ channel inactivation between sensory and motor fibres might be due to a different redox status of the channel protein.

Correspondence to: S. Quasthoff, Department of Neurology, Technical University Munich, Möhlstrasse 28, D-81675 München, Germany

A

sensory axon
$\tau_{h1} = 0.40$ ms

$\tau_{h1} = 0.52$ ms
motor axon

sensory axon
$\tau_{h1} = 0.58$ ms

$\tau_{h1} = 0.52$ ms $\tau_{h2} = 1.56$ ms
motor axon

sensory axon
$\tau_{h1} = 0.86$ ms

$\tau_{h1} = 1.0$ ms $\tau_{h2} = 3.9$ ms
motor axon

10 pA
6 ms

B

cell attached
○ τ_{h1} sensory axon
● τ_{h1} motor axon
▲ τ_{h2} motor axon

C

cell attached
○ sensory axon
■ motor axon

Fig. 1A–C. Differences in inactivation of Na^+ channels from rat sensory and motor axons. **A** Superimposed are recordings from one paranodally demyelinated rat dorsal root (sensory) and one ventral root (motor) axon. Multi-channel Na^+ currents were obtained using patch pipettes in the axon-attached mode. Na^+ currents were induced by changing the membrane potential from -100 mV to the indicated potentials (averaged currents from ten identical voltage steps; automatic subtraction of leakage and ca-

pacitive currents by means of a prepulse protocol). **B** Fitted time constants τ_h plotted as a function of membrane potential. Data were obtained from 12 patches on sensory and 17 patches on motor axons in the axon-attached mode. **C** Amplitude factor $1-g$ of the slow phase of Na^+ inactivation plotted against membrane potential. Data were obtained from 12 patches on sensory and 17 patches on motor axons. ***, Extremely significant; $P < 0.001$; **, very significant, $P < 0.01$; *, significant, $P < 0.05$

Materials and methods

Preparations. Male Wistar rats, weighing 300–400 g, were obtained from Thomae, Biberach, Germany. The animals were anaesthetized with urethane (1.5 g/kg, i.p., supplemented as required) for a laminectomy to expose the cauda equina and the spinal ganglia. Spinal roots were removed in their entire length (from the spinal cord to the spinal nerve). The anatomical relationship of the isolated roots to the spinal ganglia enabled us to differentiate between dorsal and ventral roots. Ventral roots (i.e. motor fibres) and dorsal roots (i.e. sensory fibres) were separately transferred into culture dishes. Enzymatic dissociation and paranodal demyelination were performed as described by Strupp et al. [24].

Solutions. Multi- and single-channel recordings were performed in a bathing solution of the following composition (in mM): CsCl 145, $CaCl_2$ 0.46, $MgCl_2$ 1.18, EGTA 1.0, HEPES 10, pH 7.2 (adjusted with NaOH). The pipette solution contained (in mM): sodium gluconate 150, $CaCl_2$ 2.2, $MgCl_2$ 1.2, HEPES 10, pH 7.4. The reduced form of glutathione (GSH) was obtained from Sigma. The pH of the glutathione-containing solutions was adjusted with CsOH to 7.2. Glutathione was added to the bathing solution via a multi-pipette array positioned close to the patch pipette.

Fluorescence staining of axons with monochlorobimane. Ca^{2+} free Ringer solution with a 40 μM solution of the highly glutathione-specific dye monochlorobimane (MBCL) [20] was added to the dishes containing sensory or motor axons. Nerve fibres were incubated at 37°C for 90 min for loading the axons with MBCL. The solution with MBCL was washed out and axons were perfused with normal Ca^{2+}-free Ringer solution. The phase-contrast and fluorescence images were performed within the next 60 min on a Zeiss Axiovert M 35 microscope equipped for fluorescence microscopy. The following filter combination was used: bandpass 395–440 nm (excitation); dichroic mirror Zeiss FT 460; cut off filter 470 nm (emission).

Data recording and analysis. Experiments were performed at room temperature (22°C) by means of standard patch-clamp techniques [7]. Patch pipettes were drawn by a DMZ puller (Zeitz, Augsburg, Germany) from borosilicate glass tubings (GC 150 TF-10, Clark Electromedical Instruments, Pangbourne, UK), coated with Sylgard and fire-polished immediately before the experiment. The pipettes had resistances between 15 MΩ and 20 MΩ. Recordings were made with an Axopatch 200 amplifier (Axon Instruments, Foster City, Calif., USA); the current signals were filtered with its internal 5-kHz filter and digitized at a sampling rate of 10 kHz. The data were stored on an optical disc memory system and analysed using a Tandon 386/33 computer and pClamp 5.5 software (Axon Instruments). The current traces shown in the plots were low-pass filtered with the Gaussian filter of the pClamp 5.5 software at 2 kHz. Multi-channel recordings of macroscopic Na^+ currents were averaged from ten identical voltage steps; leakage and capacitive currents were automatically subtracted by means of a prepulse protocol. Single-channel recordings of late or background Na^+ currents were recorded during a 15-s-long interval immediately after the voltage step from the holding potential to a given membrane potential. Patch-clamp recordings were made on the nodal/paranodal area of axonal segments of enzyme-treated fibres (see above). The experiments were performed in the axon-attached or excised inside-out configuration and results are based on observations on 63 patches. Averaged data are expressed as means ± SEM. Inward currents are illustrated as downward deflections.

Results

Differences in inactivation of Na^+ channels from sensory and motor axons

Figure 1A illustrates multi-channel Na^+ current recordings from the nodal/paranodal area of peripheral rat
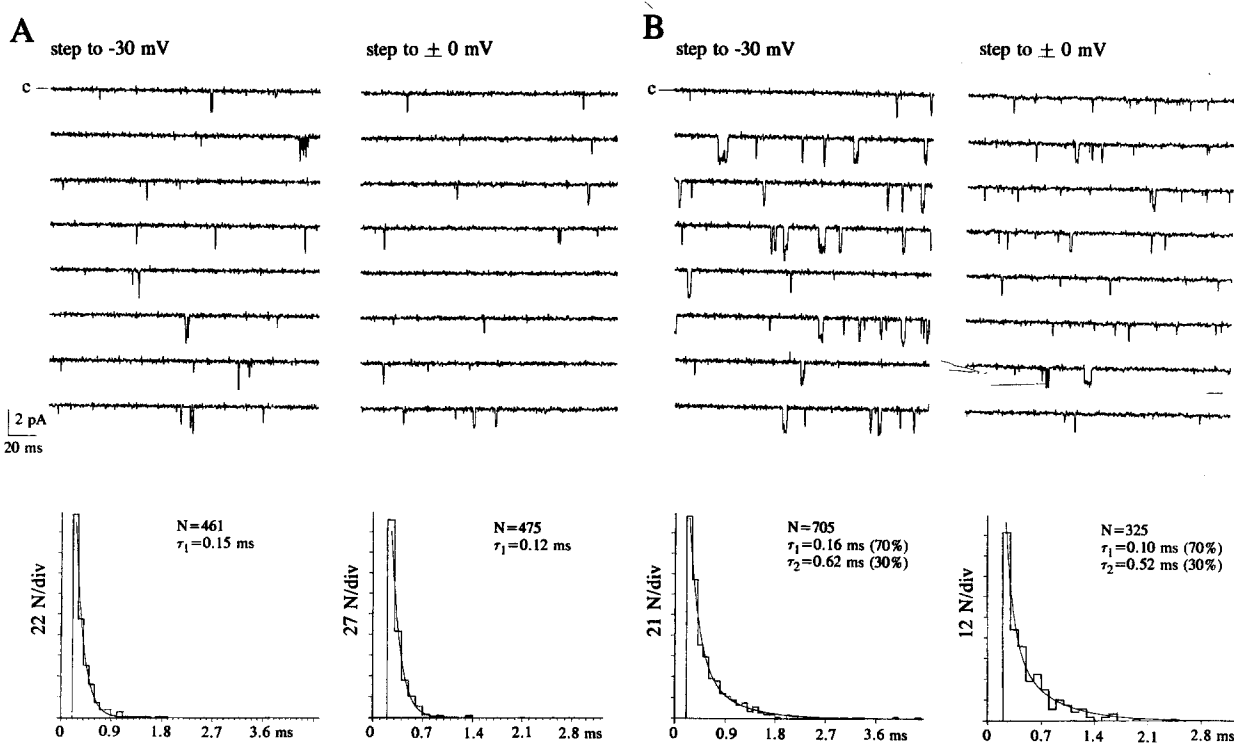
Fig. 2 A, B. Single-channel late or background Na^+ currents in rat sensory and motor axons. **A** Single Na^+ channel current activity from an axon-attached patch on a sensory axon was observed for 15 s following a change in the membrane potential from -100 to -30 and to 0 mV. The open-time histograms were determined for the 15 s of recording as illustrated in the insets (N, number of events). **B** Single Na^+ channel current activity from an axon-attached patch on a motor axon. The same recording protocol was used as in **A** (illustrated current traces are filtered with 2 kHz)

axons. Superimposed are axon-attached recordings from one sensory and one motor axon. Na^+ channel currents were induced by changing the membrane potential from -100 mV to 0, -20, and -40 mV. The decay of inward currents is clearly slower in motor as compared to sensory axons. This difference in inactivation was more marked at negative membrane potentials. The time course of inactivation was measured by fitted exponentials to quantify the differences seen between sensory and motor axons. The inactivation variable, h, of the Na^+ currents in sensory and motor axons was fitted by the sum of two exponentials:

$$h = g \exp\left(-t/\tau_{h1}\right) + (1-g) \exp\left(-t/\tau_{h2}\right),$$

where t is the time elapsed from the beginning of the depolarizing potential step, τ_{h1} and τ_{h2} are the time constants of inactivation, and g and $1-g$ are the amplitudes of both exponentials. For the sensory axons, Na^+ channel inactivation in the axon-attached configuration was best fitted with a single exponential since the amplitude $(1-g)$ of the second component was always smaller than 1% of the amplitude g of the first time constant. In contrast, patches from motor axons in the cell-attached mode always exhibited two inactivation phases for voltage steps from the holding potential (-100 mV) to potentials more negative than 0 mV. The first time constant (τ_{h1}) was similar in sensory and motor axons for a given potential. The second time constant (τ_{h2}) for motor axons increased with more negative membrane potentials. Figure 1 B summarizes these findings by showing the fitted

time constants τ_{h1} and τ_{h2} for sensory and motor axons as a function of the membrane potential. The data represent axon-attached recordings from 12 sensory and 17 motor axons. The mean values $\pm$ SEM of τ_{h1} and τ_{h2} are given. The fast component and the slow component of inactivation exhibited a clear voltage dependence, with longer time constants at negative and shorter time constants at positive membrane potentials. However, sensory fibres did not show bi-exponential kinetics of inactivation. Figure 1 C shows the amplitude factor $1-g$ of the slow component in motor axons plotted against the membrane potential. This parameter was also voltage-dependent. It increased from 0.045 at -20 mV to 0.12 at -40 mV. In contrast to motor axons, $1-g$ in sensory axons was always smaller than 0.01.

Another difference in the kinetics of Na^+ channel inactivation of sensory and motor axons in the axon-attached configuration was revealed in open-time histograms and mean open-time analyses from late or background currents (in the terminology of Patlak and Ortiz [18]). Late Na^+ currents in the node of Ranvier were first described by Dubois and Bergman on voltage-clamped sensory and motor fibres in the frog [5]. In the present study, such currents were analysed using single-channel events recorded for 15 s following voltage steps from the holding potential of -100 mV to potentials ranging from -40 mV to $+20$ mV (in steps of 10 mV). Figure 2 A shows characteristic current traces from an axon-attached patch of a sensory axon after voltage steps to membrane potentials of -30 mV and 0 mV and their

A

B
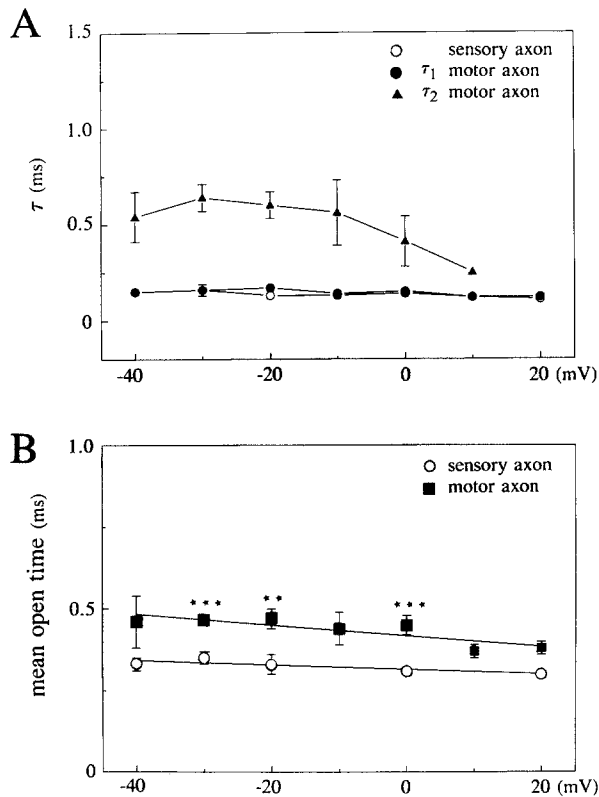
Fig. 3 A, B. Differences between sensory and motor axons in fitted open and mean open times of late Na^+ channel currents. **A** Fitted open-time τ of sensory and motor axons as a function of membrane potential. Late Na^+ channel recordings as shown in Fig. 2 were analysed (data are from 10 axon-attached recordings on sensory and from 17 such recordings on motor axons). **B** Mean open times determined from the same recordings as used in **A** as a function of membrane potential. Differences in mean open times of sensory and motor axons are significant (***, $P < 0.001$) at -30 mV and 0 mV and significant at -20 mV (**, $P < 0.01$)

corresponding fitted open-time histograms. A uniform distribution of short voltage-independent openings was found at -30 mV and 0 mV. Occasional clustered short openings of tens of sequential unitary inward currents were seen, similar to the bursts observed in frog muscle [18] (not illustrated). The calculated open-time histogram for sensory axons at a given potential was fitted with one short time constant τ_1 (Fig. 2 A). In contrast, late Na^+ currents from motor axons in the axon-attached mode, as shown in Fig. 2 B, revealed a bi-exponential distribution of short and long-lasting open times. The contribution of the amplitude of the slow component τ_2 in the open-time histograms never exceeded 30% of the total amplitude.

Figure 3 A summarizes differences in the fitted open times between sensory (one time constant) and motor axons (two time constants). The time constants of the short openings were similar in both axon types over the whole potential range investigated and were not voltage-dependent. The time constant of the long openings from motor axons showed a moderate, bell-shaped voltage dependence with a maximum around -30 mV. Also differ-

ent in sensory as compared to motor axons were the mean open times of the single Na^+ channel currents. This is illustrated in Fig. 3 B. The mean open time of Na^+ channels in sensory axons was significantly shorter as compared to motor axons in the voltage range from -40 mV to 0 mV. On the other hand, single-channel Na^+ current amplitudes (sensory: 1.34 ± 0.02 pA at -30 mV and 0.90 ± 0.06 pA at 0 mV versus motor: 1.38 ± 0.04 pA at -30 mV and 0.95 ± 0.08 pA at 0 mV) and slope conductance were not significantly different in sensory (12.5 ± 0.4 pS) as compared to motor (13.1 ± 0.6 pS) axons (plot not shown). Unitary current amplitude and slope conductance were within the range of other vertebrate Na^+ channels [8, 14].

Effect of glutathione on Na^+ channel inactivation of sensory and motor axons

On the basis of analyses of Na^+ channel kinetics in excised membrane patches from rat axons previously described by Strupp et al. [24], we applied the reducing agent glutathione (3 mM) to excised membrane patches (inside-out configuration) of sensory and motor axons (Fig. 4 A, B). Glutathione accelerated Na^+ channel inactivation by changing the kinetics from a process with two time constants to a current decline with single-exponential decay. Thereby time constants of inactivation of sensory and motor axon Na^+ channels became nearly identical at corresponding membrane potentials. The amplitudes of the multi-channel peak Na^+ currents remained unchanged in the presence of GSH. Figure 5 summarizes the findings on 12 patches from sensory and on 14 patches from motor axons. In this plot the fitted time constants τ_{h1} and τ_{h2} of patches in the excised inside-out mode are presented as a function of the membrane potential. The slow time constant of inactivation seen in motor as well as sensory axons was completely absent after GSH had been added to the bathing solution around the patch pipette whereas the fast component of inactivation was slightly accelerated.

In another series of experiments, the effects of GSH on late, single-channel Na^+ currents in sensory and motor axons were tested. In contrast to axon-attached recordings, Na^+ channels in patches from sensory and motor axons in the excised inside-out mode showed no clear differences in their gating behaviour (Fig. 6 A, B, left side). Under these conditions late Na^+ currents from both types of fibres revealed short and long openings, which were fitted by two exponentials. The relative contribution of both components was similar in sensory and motor axons, i.e. $60-70\%$ were short openings. Addition of GSH to the bathing solution suppressed the long-lasting single-channel openings seen in excised membrane patches. This is illustrated in the right part of Fig. 6 A, B. In addition, GSH (3 mM) reduced the total number of single-channel events from 1179 to 600 in a patch from a sensory axon (Fig. 6 A) and from 621 to 315 in a patch from a motor axon (Fig. 6 B). The remaining events consisted of short single-channel openings
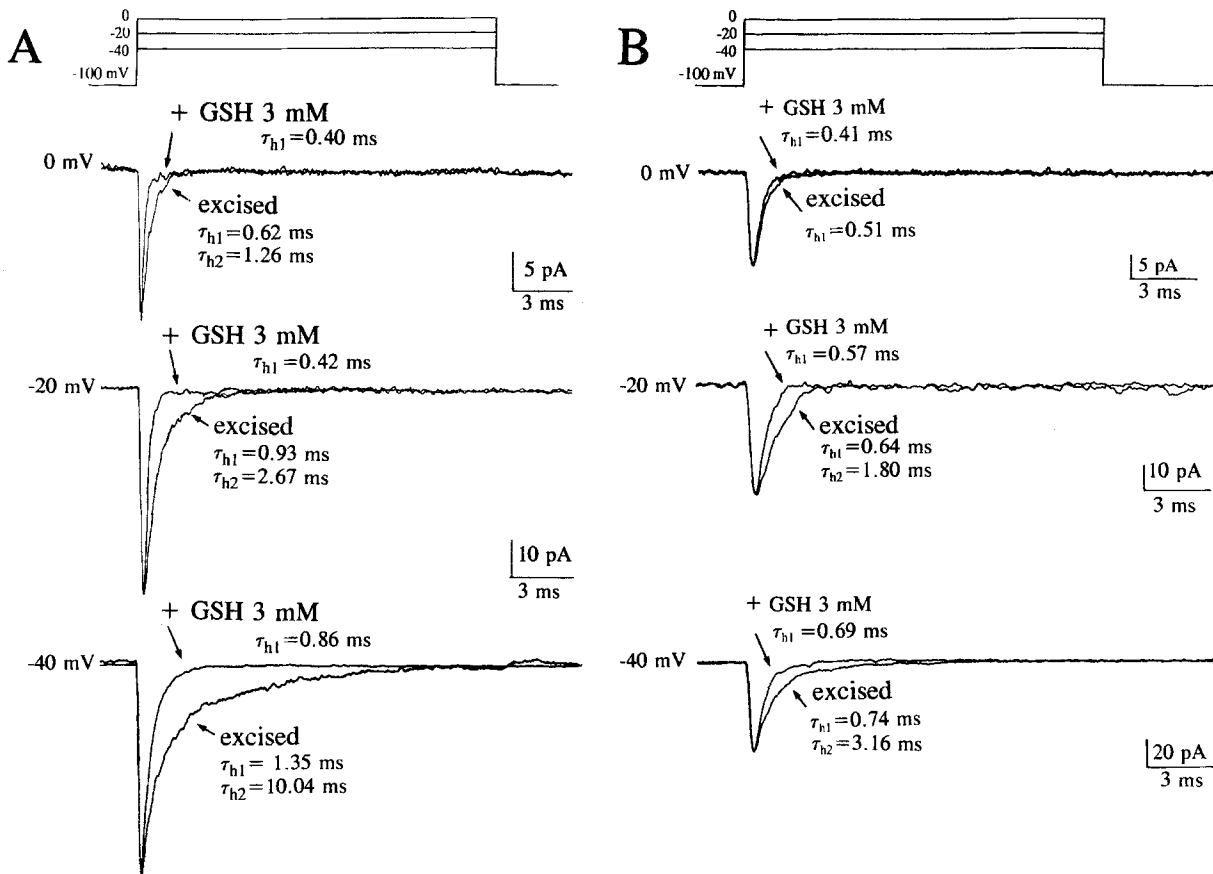
Fig. 4 A, B. Effects of glutathione on inactivation behaviour of excised patches from sensory and motor axons. The figure shows multi-channel recordings obtained with patch pipettes from paranodally demyelinated rat dorsal and ventral root axons in the excised inside-out mode. Na^+ currents were induced by changing the membrane potential from -100 mV to the indicated potentials (averaged currents from ten identical voltage steps; automatic subtraction of leakage and capacitive currents by means of a prepulse protocol). A Voltage steps were performed on an excised sensory axon membrane before and after the application of glutathione (GSH, 3 mM). GSH was applied to the cytoplasmic face of the membrane. The time constant(s) of inactivation (τ_h) were determined by fitting one or two exponentials. B The same experimental protocol was performed on an excised membrane patch from a motor axon

that were best described by an open-time histogram with one fitted exponential τ_1.

It is well known that iodate, an oxidizing agent, slows down inactivation of axonal Na^+ currents [23, 27]. Therefore, we were interested to test the interactions of iodate with the reducing agent GSH on the inactivation kinetics of Na^+ currents in axonal membrane patches. In the experiment illustrated in Fig. 7, a multi-channel Na^+ current from an excised inside-out patch from a sensory fibre was recorded. Inactivation proceeded bi-exponentially with two time constants τ_{h1} and τ_{h2} at -40 mV. Application of GSH (2 mM) to the bathing solution accelerated inactivation to a single-exponential time course with only one time constant τ_{h1}. Addition of iodate (1 mM) to the GSH-containing solution antagonized the effects of glutathione. Inactivation was strongly slowed down to a process with at least two time constants. We also made the opposite observation: GSH added to an excised inside-out patch with iodate present on the cytoplasmatic side accelerated Na^+ current inactivation (not illustrated).

Finally, we tried to find evidence for the presence of GSH in rat spinal root axons. According to Rice et al. [20], green fluorescence is produced when monochlorobimane (MBCL) is excited at 395 nm in the presence of GSH. After incubation of demyelinated rat sensory and motor axons with MBCL (40 µM) for 60−90 min at 37°C, we were able to observe fluorescence under the conditions described above. Figure 8 shows a nodal/paranodal demyelinated dorsal root axon after MBCL incubation. Demyelinated nodal and paranodal areas of the axon displayed fluorescence. Under identical incubating procedures, both types of axon displayed an intra-axonal level of GSH (concentration higher than 500 µM) as estimated by fluorescence. As we were unable to perform flow cytometry we took pictures in order to compare the GSH concentration in sensory and motor axons from stained sensory and motor axons in a standard procedure. Sensory axons seemed to have a higher intracellular GSH concentration compared to motor axons, when the intensity of fluorescence was taken as an indicator for GSH concentration. However, our photographic
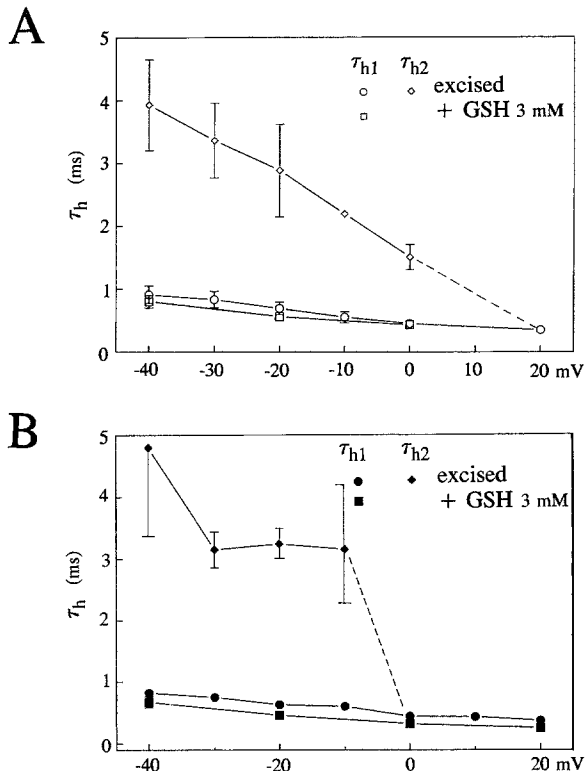
Fig. 5A, B. Time constants of inactivation (τ_h) before and after the application of GSH on sensory and motor axons. **A** Multi-channel recordings shown in Fig. 4 from sensory axons before and after application of GSH were fitted with one or two exponentials to determine the inactivation time course. The time constants are plotted as a function of the membrane potential. Mean values ± SEM from 12 excised inside-out patches are shown. **B** Fitted time constants, τ_h, of motor axon patches before and after application of GSH. The plot summarizes data obtained from 14 excised, inside-out patches

method did not allow us to quantify numerically the absolute or relative GSH concentration in sensory and motor axons.

Discussion

Differences in inactivation of Na^+ channels from sensory and motor axons

Na^+ current inactivation of mammalian sensory and motor axons were analysed by means of single- and multi-channel patch-clamp recordings. Observations from axon-attached patches revealed Na^+ current inactivation with a fast time constant in both sensory as well as motor fibres. However, motor fibres showed a second, slow inactivation process at potentials between − 40 mV and 0 mV.

A second-order process of Na^+ current inactivation has been previously described in amphibian motor as well as sensory myelinated axons [1, 4, 22]. The main difference between sensory and motor nerve fibres was the relative contribution of the fast and slow phase to the process of inactivation [22]. Motor fibres showed a

uniform ratio of the fast and slow phases of inactivation over the investigated voltage range, while in sensory fibres the amplitude of the slow phase decreased at more depolarized potentials. Our data from rat fibres differ in two aspects from these observations. First, slow inactivation was not found in sensory axons in the cell-attached mode of the patch-clamp technique. Second, motor axon Na^+ channel inactivation had a slow phase only at membrane potentials negative to 0 mV while in the experiments on frog nerves by Schwarz et al. [22] a slow phase was still observed at + 40 mV. These discrepancies might be due to the animal species examined (amphibian versus mammalian axons) and/or to the methods used (clamp of a complete Ranvier node versus patch clamp of a small membrane area [16, 22]). The holding potential in the cell-attached mode of the patch-clamp method, on the other hand, is set more negative (− 100 mV) than the normal resting potential of a myelinated axon in order to activate a sufficient number of Na^+ channels. It is also known that the giga-seal formation itself alters inactivation parameters of the Na^+ channels [6].

In addition to the multi-channel macroscopic Na^+ currents the patch-clamp technique enabled us to investigate differences between sensory and motor axon, late, single Na^+ channel events. Dubois and Bergman [5] first described a late Na^+ current in the frog node of Ranvier. They found that a small fraction of Na^+ channels failed to inactivate during long-lasting depolarizing pulses leading to a late Na^+ current that appeared to be more marked in sensory than in motor fibres. Similar currents were later observed with the patch-clamp technique by Patlak and Ortiz [18] in frog skeletal muscle. The analysis of these late Na^+ currents in the present study revealed differences in the open-time histogram fits and calculated mean open times between sensory and motor axons. Sensory axons showed short openings with one fitted time constant while motor axons had short and longer lasting openings. Mean open times of sensory and motor axons were also significantly different. These findings are in contrast to the observation of Dubois and Bergman [5] who found the late Na^+ current mainly on sensory fibres. However, the contribution of late currents to the total Na^+ inward current is small (between 1% and 5% of the total current).

Effects of glutathione on Na^+ channel inactivation of sensory and motor axons

As described by many authors [10, 17, 24], slowing of the inactivation behaviour of Na^+ channels can occur following membrane excision or after pharmacological modification of Na^+ channels (for review see [27]). Since a transition from the cell-attached to the excised inside-out mode of sensory and motor axons patches blurred the differences between sensory and motor axon Na^+ inactivation, it seems as if a cytoplasmic factor might control Na^+ channel inactivation and cause the differences seen between sensory and motor axons in cell-attached patches. Some possible factors in this re-
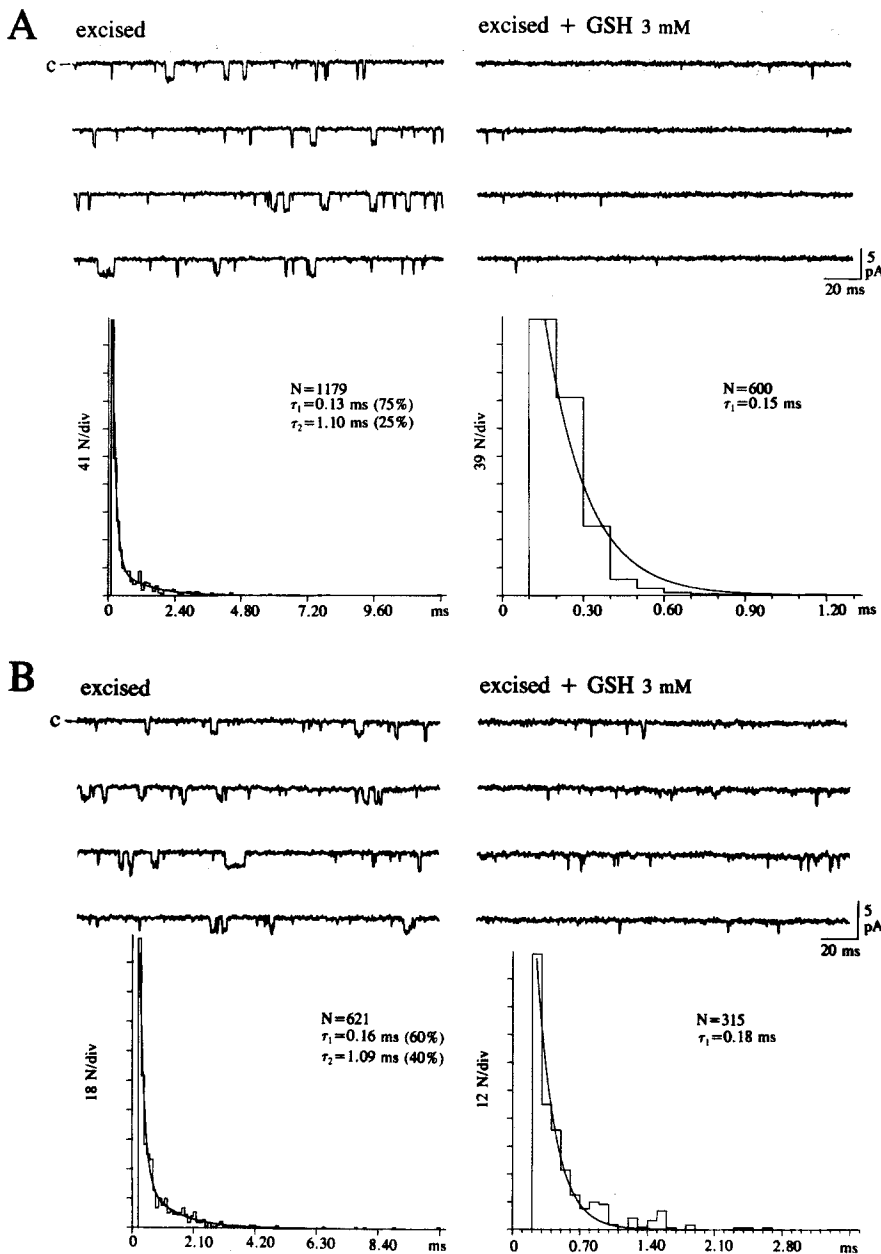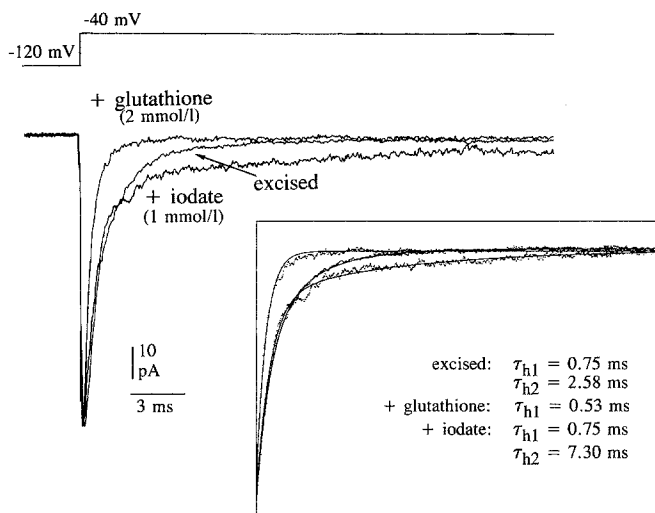
Fig. 6A, B. Effects of GSH on sensory and motor axon late Na^+ currents. **A** Representative traces of single Na^+ channel current activity from an excised, inside-out patch of a sensory axon before and after application of 3 mM GSH to the bathing solution. The Na^+ channel events were observed for 15 s following a change in the membrane potential from -100 mV to -30 mV. Open-time histograms were determined during these 15 s of recording. **B** Single Na^+ channel current activity from an excised, inside-out patch of a motor axon. The same recording protocol was used as in **A** (illustrated current traces are filtered with 2 kHz)

spect (for review see [3, 17]) are phosphorylation, coupling to G proteins, protein kinase C interaction and metabolites of the glycolytic pathway [11]. These factors are not likely to explain our findings since addition of the corresponding substances to an excised inside-out patch often caused a reduction in Na^+ current peak amplitude and a slowing in inactivation (for review [3]). Glutathione is another possible link between cellular metabolism and functional activity of Na^+ channels. This peptide may alter the mobility of the channel protein by modification of disulphide bonds between cysteine residues. Such a model has been proposed by Ruppersberg et al. [21] for voltage-gated K^+ channels. However, the region between repeats III and IV of the Na^+ channel α subunit, which is known to be important for the inactivation process [3], does not contain cysteine [25, 28]. Cysteine residues in several other peptide segments have not been claimed to be responsible for alter-

ation in inactivation kinetics. Another possible site of action for glutathione might be the disulphide bond between the α and the $\beta2$ subunits of the channel protein. However, the importance of the $\beta2$ subunit for inactivation has not been studied in detail [3]. Coexpression of the α and $\beta1$ subunits, on the other hand, accelerates the decay of Na^+ channel inactivation [9].

A further possibility to explain the differences in Na^+ current inactivation kinetics between sensory and motor axons could be the existence of different populations of Na^+ channels as suggested by Dubois and Bergman [5]. In fact, it was found in the central nervous system that a Na^+ channel subtype RI is expressed in the neuronal cell body whereas subtypes RII and RIII are expressed on the dendrites [29]. Little is known about the expression pattern of Na^+ channel subtypes in mammalian myelinated axons of the peripheral nervous system [3]. However, two different Na^+ channel popu-

460

-40 mV
-120 mV

+ glutathione
(2 mmol/l)

+ iodate
(1 mmol/l)

excised

10
pA

3 ms

excised:	τ_{h1}	= 0.75 ms
	τ_{h2}	= 2.58 ms
+ glutathione:	τ_{h1}	= 0.53 ms
+ iodate:	τ_{h1}	= 0.75 ms
	τ_{h2}	= 7.30 ms

Fig. 7. Effect of iodate on Na^+ current inactivation. The figure shows multi-channel recordings obtained with patch pipettes from paranodally demyelinated rat dorsal root axons in the excised, inside-out mode. Na^+ currents were induced by changing the membrane potential from -120 mV to -40 mV (averaged currents from ten identical voltage steps; automatic subtraction of leakage and capacitive currents by means of a prepulse protocol). Voltage steps were performed on an excised, sensory axonal membrane before and after the application of glutathione (2 mM) and iodate (1 mM). GSH and iodate were applied to the cytoplasmic face of the membrane. The time constant(s) of inactivation (τ_h) were determined by fitting one or two exponentials

lations could explain the reduction of the total number of events oberserved in the presence of glutathione. One population would be responsible for the fast component of the inactivation phase (not sensitive to GSH), the second population for the slow component of the inactivation process (GSH-sensitive). In this case, differences in Na^+ inactivation between sensory and motor axons could be explained by a different expression pattern of Na^+ channel subtypes in sensory and motor axons. However, differences in Na^+ current inactivation and single-channel gating behaviour are not necessarily due to two different Na^+ channel subtypes [12]. Recent studies have shown that individual Na^+ channels expressed from a single clone can switch between different gating modes. Cloned Na^+ channel subtypes RIII and μI occasionally failed to inactivate and showed prolonged bursting and long openings [26, 30].

A heterogeneous distribution of GSH has been found in the nervous system of the rat [19]. However, up to now there has been no quantitative study of GSH concentration in sensory and motor axons of the peripheral nervous system. Philbert et al. [19], using mercury orange and o-phthaldialdehyde histofluorescence staining, found GSH in sensory nerve cell bodies of lumbar dorsal root ganglia, while the large motor nerve cell bodies in the lumbar spinal cord displayed almost no detectable fluorescence. In our staining experiments, enzymatically dissociated and demyelinated sensory and motor axons displayed fluorescence when stained with the GSH-
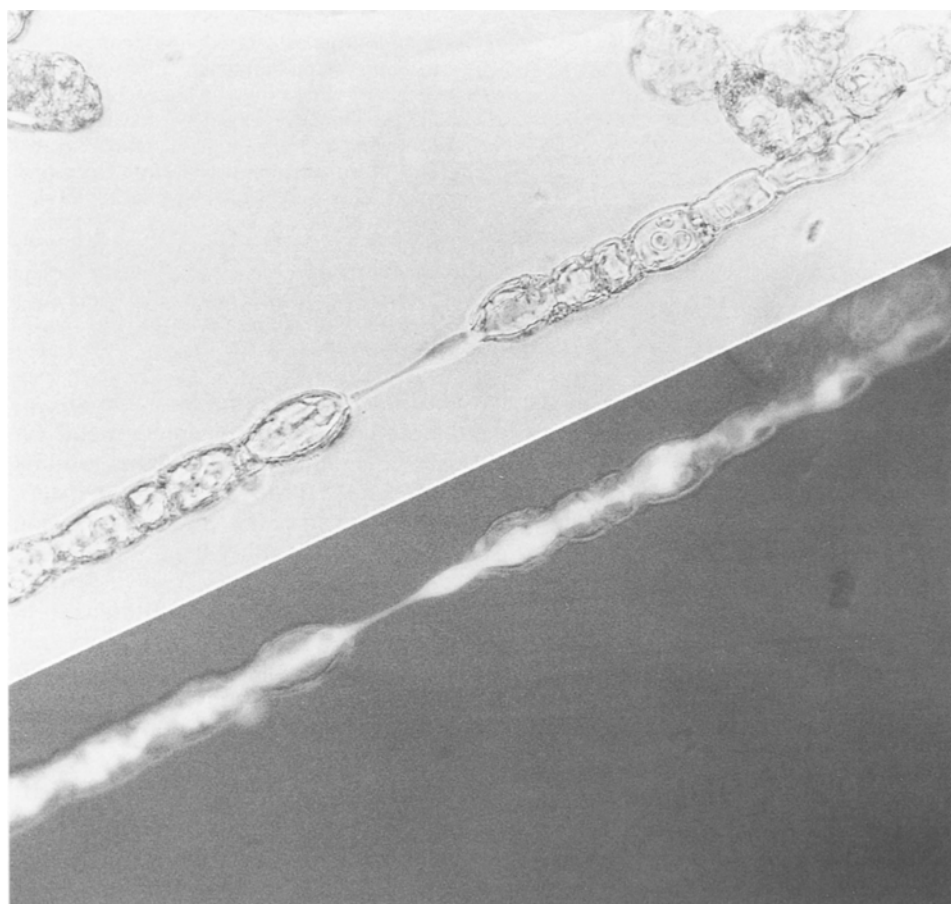
Fig. 8. Monochlorobimane staining of a dorsal root axon. Phase-contrast (*above*) and fluorescence (*below*) images of a nodal/paranodal demyelinated dorsal root axon incubated with 40 μM monochlorobimane. Note the slight, uniform fluorescence of the demyelinated nodal and paranodal section of the axon. Original magnifications: $\times 320$

specific dye monochlorobimane. The intensity of fluorescence indicated a higher concentration of GSH in sensory fibres as compared to motor fibres. However, for technical reasons, we were not able to express the difference in the concentration of GSH in these two types of axons quantitatively.

In conclusion, the modulation of Na⁺ channel gating by glutathione is an example for the coupling of axonal metabolism to Na⁺ channel activity. Such metabolic factors may also contribute to other differences in the membrane conductances of sensory and motor axons.

References

1. Benoit E, Corbier A, Dubois JM (1985) Evidence for two transient Na⁺ currents in the frog node of Ranvier. J Physiol (Lond) 361:339–360
2. Bretag AH, Stämpfli R (1975) Differences in action potentials and accommodation of sensory and motor myelinated nerve fibres as computed on the basis of voltage clamp data. Pflügers Arch 354:257–271
3. Catterall WA (1992) Cellular and molecular biology of voltage-gated Na⁺ channels. Physiol Rev 72 [Suppl 4] S15–S48
4. Chiu SY (1976) Inactivation of sodium channels: second order kinetics in myelinated nerve. J Physiol (Lond) 273:573–596
5. Dubois JM, Bergman C (1975) Late sodium current in the node of Ranvier. Pflügers Arch 357:145–148
6. Fahlke Ch, Rüdel R (1991) Giga-seal formation alters properties of sodium channels of human myoballs. Pflügers Arch 420:248–254
7. Hamill, OP, Marty A, Neher E, Sakmann B, Sigworth FJ (1981) Improved patch-clamp techniques for high resolution current recording from cells and cell-free membrane patches. Pflügers Arch 391:85–100
8. Jonas P, Bräu ME, Hermsteiner M, Vogel W (1989) Single-channel recording in myelinated nerve fibers reveals one type of Na channel but different K channels. Proc Natl Acad Sci USA 86:7238–7242
9. Isom LL, De Jongh KS, Reber BFX, Offord J, Charbonneau H, Walsh K, Goldin AL, Catterall WA (1992) Primary structure and functional expression of the β1 subunit of the rat brain sodium channel. Science 256:839–842
10. Kohlhardt M (1991) Gating properties of cardiac Na⁺ channels in cell-free conditions. J Membr Biol 122:11–21
11. Kohlhardt M, Fichtner H, Fröbe U (1989) Metabolites of the glycolytic pathway modulate the activity of single cardiac Na⁺ channels. FASEB J 3:1963–1967
12. Moorman JR, Kirsch GE, VanDongen AMJ, Joho RH, Brown AM (1990) Fast and slow gating of sodium channels encoded by a single mRNA. Neuron 4:243–252
13. Neumcke B (1981) Differences in electrophysiological properties of motor and sensory nerve fibres. J Physiol (Paris) 77:1135–1138
14. Neumcke B (1990) Diversity of sodium channels in adult and cultured cells, in oocytes and in lipid bilayers. Rev Physiol Biochem Pharmacol 115:1–49
15. Neumcke B, Schwarz W, Stämpfli R (1980) Differences between K channels in motor and sensory nerve fibres of the frog as revealed by fluctuation analysis. Pflügers Arch 387:9–16
16. Nonner W (1969) A new voltage clamp method for Ranvier nodes. Pflügers Arch 309:116–192
17. Patlak J (1991) Molecular kinetics of voltage-dependent Na⁺ channels. Physiol Rev 71:1047–1080
18. Patlak JB, Ortiz M (1986) Two modes of gating during late Na⁺ channel currents in frog sartorius muscle. J Gen Physiol 87:305–326
19. Philbert MA, Beiswanger CM, Waters DK, Reuhl KR, Lowndes HE (1991) Cellular and regional distribution of reduced glutathione in the nervous system of the rat: histochemical localization by mercury orange and o-phthaldialdehyde-induced histoflurescence. Toxicol Appl Pharmacol 107:215–227
20. Rice GC, Bump EA, Shrieve DC, Lee W, Kovacs M (1986) Quantitative analysis of cellular glutathione by flow cytometry utilizing monochlorobimane: some applications to radiation and drug resistance in vitro and in vivo. Cancer Res 46:6105–6110
21. Ruppersberg JP, Stocker M, Pongs O, Heinemann SH, Frank R, Koenen M (1991) Regulation of fast inactivation of cloned mammalian I_K (A) channels by cysteine oxidation. Nature 352:711–714
22. Schwarz JR, Bromm B, Spielmann RP, Weytjens LF (1983) Development of Na inactivation in motor and sensory myelinated nerve fibres of Rana esculenta. Pflügers Arch 398:126–129
23. Stämpfli R (1974) Intraaxonal iodate inhibits sodium inactivation. Experientia 30:505–508
24. Strupp M, Quasthoff S, Mitrović N, Grafe P (1992) Glutathione accelerates sodium channel inactivation in excised rat axonal membrane patches. Pflügers Arch 421:283–285
25. Stühmer W, Conti F, Suzuki H, Wang X, Noda M, Yahagi N, Kubo H, Numa S (1989) Structural parts involved in activation and inactivation of the sodium channel. Nature 339:597–603
26. Ukomadu C, Zhou J, Sigworth FJ, Agnew WS (1992) μI Na⁺ channels expressed transiently in human embryonic kidney cells: biochemical and biophysical properties. Neuron 8:693–676
27. Ulbricht W (1990) The inactivation of sodium channels in the node of Ranvier and its chemical modification. In: Narahashi T (ed) Ion channels, vol 2. Plenum Press, New York, pp 123–168
28. Vassilev PM, Scheuer T, Catterall WA (1988) Identification of an intracellular peptide segment involved in sodium channel inactivation. Science 241:1658–1661
29. Westenbroek RE, Merrick DK, Catterall WA (1989) Differential subcellular localization of RI and RII Na⁺ channel subtypes in central neurons. Neuron 3:695–704
30. Zhou J, Potts JF, Trimmer JS, Agnew WS, Sigworth FJ (1991) Multiple gating modes and the effects of modulating factors on the μI sodium channel. Neuron 7:775–785